Journal of Asian Ceramic Societies 4 (2016) 219–233

HOSTED BY

Contents lists available at ScienceDirect

Journal of Asian Ceramic Societies

journal homepage: www.elsevier.com/locate/jascer

Review Article

Review on the elaboration and characterization of ceramics refractories based on magnesite and dolomite

Chaouki Sadik[a,*], Omar Moudden[b], Abdselam El Bouari[a], Iz-Eddine El Amrani[c]

[a] Laboratory of Physical Chemistry of Applied Materials (LPCMA), Department of Chemistry, Faculty of Sciences Ben Msik, University Hassan II, Casablanca, Morocco
[b] Laboratory of Structure and Rehabilitation (LSR), Casablanca, Morocco
[c] Department of Earth Sciences, Geomaterials and Geo-Environment Team (Geo M&E), Scientific Institute, University Mohammed V, Rabat, Morocco

ARTICLE INFO

Article history:
Received 29 April 2016
Received in revised form 13 June 2016
Accepted 25 June 2016
Available online 11 July 2016

Keywords:
Dolomite
Magnesite
Firing
Ceramics

ABSTRACT

One of the most important elements of furnaces, boilers and other heating units is the structure (lining), usually made of silica–alumina, basic or special refractories. The basic refractories are materials that are increasingly in demand and whose manufacturing involves necessarily the use of MgO and CaO. In this article, the description and characterization of magnesite ($MgCO_3$) and dolomite ($Mg,Ca(CO_3)_2$) and their contribution in industrial ceramics-refractories have been reviewed.

Contents

1. Introduction

Different mixtures of geomaterials (kaolin clay, red clay, marl, andalusite, perlite, pozzolana, schist, silica sand, magnesite, forsterite, etc.), and additives (natural and synthetic) are used for the elaboration of ceramics and refractories [1]. These industrial minerals and rocks are the raw materials of economic value that are not classified as metallic minerals, fossil fuels or precious stones.

Shaped and unshaped basic ceramics-refractories, based on magnesite and dolomite are produced worldwide for lining industrial furnaces, especially primary and secondary steel furnaces [2]. Actually, there are two methods to produce refractory by using dolomite and magnesite as materials, one is fired in rotary or shaft kilns up to dead burning temperatures of 1500–1800 °C, the other is produced by electric smelting furnace with a temperature over 2500 °C, for example burned magnesite (i.e. fused magnesia) and electrocast spine are produced by electric smelting furnace. The behavior of these elaborated materials in high temperature has been investigated through the use of complementary methods of characterization: structural (X-ray diffraction), microstructural (scanning electron microscopy (SEM)), macroscopic (optical and polarized microscope), technological (porosity, water absorption, density, flexural strength, and shrinkage), thermal (DTA, expansion, shock, and conductivity), and chemical (resistance toward acid attack) [2].

* Corresponding author. Tel.: +212 6 45405676.
E-mail addresses: schawki37@gmail.com (C. Sadik), o.moudden@gmail.com (O. Moudden), elbouari@gmail.com (A. El Bouari), izdinelamrani@yahoo.fr (I.-E. El Amrani).

Peer review under responsibility of The Ceramic Society of Japan and the Korean Ceramic Society.

http://dx.doi.org/10.1016/j.jascer.2016.06.006

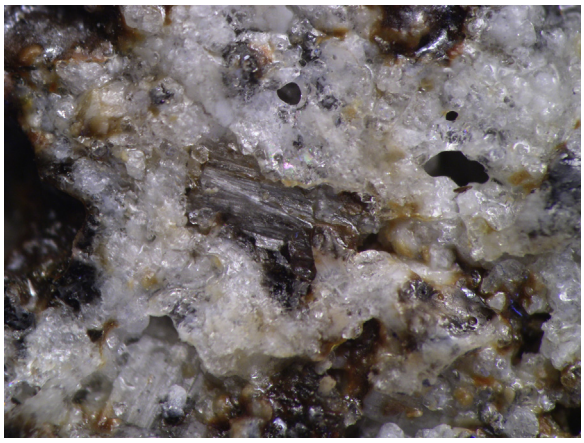

Fig. 1. Schema of the four textural elements of a refractory.

Refractory materials can be divided into several classes: chemical composition (acid, basic and special), method of implementation (shaped and unshaped), method of manufacture (fused and sintered), and porosity content (porous and dense). They are supposed to be resistant to heat and are exposed to different degrees of mechanical stress and strain, corrosion from liquids and gases, and mechanical abrasion at high temperature. The application fields of refractory are multiple and depend on the properties of each type. In fact, the performance of a refractory (good resistance to heat and thermal shock) is directly related to its texture and its richness in refractories minerals such as mullite, corundum, periclase, doloma, spinel and alumina [1]. Generally, every refractory is composed of four major structural elements that are depicted in Fig. 1 as the following; (1) aggregates (mean grain size: 1000–2500 mm) [3,4]; (2) matrix or filler materials smaller than 150 μm; (3) binder, bond, or cement; (4) pores.

The basic refractories are materials that are increasingly in demand and whose manufacture involves necessarily the synthesis of periclase, spinel and doloma. The primary attributes that make magnesia (MgO) an attractive choice are its high melting point (2800 °C) and excellent resistance to attack by iron oxides, alkalis and high lime content of flakes formed at the working temperature of steel melting furnaces [5]. Moreover, it does not suffer from issues of hydration like dolomite and lime, while also being nontoxic. Today, magnesia for refractory production is obtained from three basic sources [2] as the following: (a) natural magnesite, (b) extraction from sea water, and (c) extraction from inland brine. Basic refractories have the attributes of being relatively inexpensive compared to other bricks (special carbon refractories, zircon, zirconia, fused-cast refractory). In addition, they can be used in several applications as the following: coating of laboratory furnaces, refractory supports, thermal insulating, industrial ceramics, concrete, chemical producers and especially in the steel sector.

Several research studies have investigated the use of magnesite and dolomite in building materials and ceramics. The behavior of minerals (quartz, potassium feldspar, sodium feldspar, kaolinite, illite, calcite, dolomite, siderite, pyrite and apatite) in an improved ash fusion test was studied by Reifenstein et al. [6]. Arvanitidis [7] published a paper in 1998 on Northern Greece's industrial minerals. He studied the production and the environmental technology developments. The thermal analysis studies on the decomposition of magnesite and dolomite were studied respectively in 1993 and 1990 by Sheila [8] and Mclntosh et al. [9]. The effect of rate of heating on the decomposition reactions of some raw materials (kaolinite; $CaCO_3$; dolomite; magnesite; and mixes of these) was studied in 1984 by Ibrahim et al. [10]. In 1975, Khalifa et al. [11] studied rapid and quite reliable procedures for analysis of phosphate, quartzite and fluorspar minerals, as well as chromite, chrome–magnesite and magnesite–chrome bricks-basic refractories.

This review is intended to provide a large overview of the current status of this type of basic ceramics-refractories and to provide a summary of recent information concerning the elaboration and the characterization of refractories elaborated from magnesite and dolomite.

2. Materials

Basic refractories are manufactured using forsterite, spinel, cordierite, magnesite and dolomite. They will refer, somewhat arbitrarily, to common crystalline compounds with melting temperatures of at least 2000 °C [5]. In this work, we are interested only with magnesite and dolomite.

Magnesite is a well-known raw material widely used for making magnesia refractories. Magnesite is the mineral name for magnesium carbonate, $MgCO_3$, and was one of the original sources for magnesium oxide used in refractory products. Its theoretical composition is as follows: MgO: 47.7%; CO_2: 52.3%, with traces of Fe; Mn; Ca; Co; N and organic compounds. Magnesite is usually white or yellowish with compact appearance. It does not melt but decomposes at 700 °C. The residual MgO forms at the bottom at 2800 °C. The decomposition of magnesite in an inert N_2 atmosphere can be represented as follows: $MgCO_3 \rightarrow MgO + CO_2$.

Magnesite is delivered in three forms as the following: (1) Brute; (2) Calcined at 850 °C; (3) Dead burned and agglomerated (bricks at 1500–1800 °C). Magnesite occurs in nature in three distinct textures as the following: macrocrystalline rich in MgO (MgO content greater than 43%); microcrystalline with inclusions of dolomite (MgO content is between 39 and 43%); macrocrystalline but containing many impurities and having a MgO content of less than 39% [12].

The different methods used for the enrichment of magnesite are based on techniques such as optical or manual sorting, magnetic separation, gravity and flotation. These operations are used depending on the nature and texture of the mineral accompanying magnesite. Treatments show that the obtained concentrate has a good quality, considering the high content of MgO (exceeding 47%), and has low impurity content. The semi-industrial tests are focused on the manufacture of magnesia and magnesium sulfate from the concentrates obtained from raw magnesite.

Production of caustic magnesia and dead burned magnesia from magnesite Boudkek (north of Morocco) was carried out at 850 °C for the first and between 1650 and 1800 °C for the second. The obtained contents during these operations are as the following for the caustic magnesia: 95% MgO, 3% CaO, 0.3% Fe_2O_3, 0.12% $A1_2O_3$, and 1.2% SiO_2; and as the following for the dead burned magnesia: 96.5% MgO, 1.5% CaO, 0.6% Fe_2O_3, 0.6% $A1_2O_3$ and 0.75% SiO_2 [12].

In order to produce magnesium sulfate from magnesite, Boudkek tests were performed on representative samples whose average chemical composition is as follows: 44.16% MgO, 3.80% CaO, 0.26% Fe_2O_3, 0.35% SiO_2, 1.12% Al_2O_3 and 50.00% LoI. The treatment method is an acid attack allowing the transformation from the magnesium carbonate (magnesite) to sulfate. Three techniques were tested as the following: (1) direct attack on the raw magnesite at room temperature; (2) direct attack with heating; and (3) attack after roasting magnesite. Only the acid attack after magnesite roasting at 700 °C presents advantages, especially a coarse grain size (1 mm), and instant reaction and very high efficiency up to 99%. The obtained magnesium sulfate is of the hydrated kind ($MgSO_4 \cdot 7H_2O$) comparable to the commercial sulfate.

Dolomite is a carbonate sedimentary rock that contains more than 50% of carbonate, half of which is at least in the

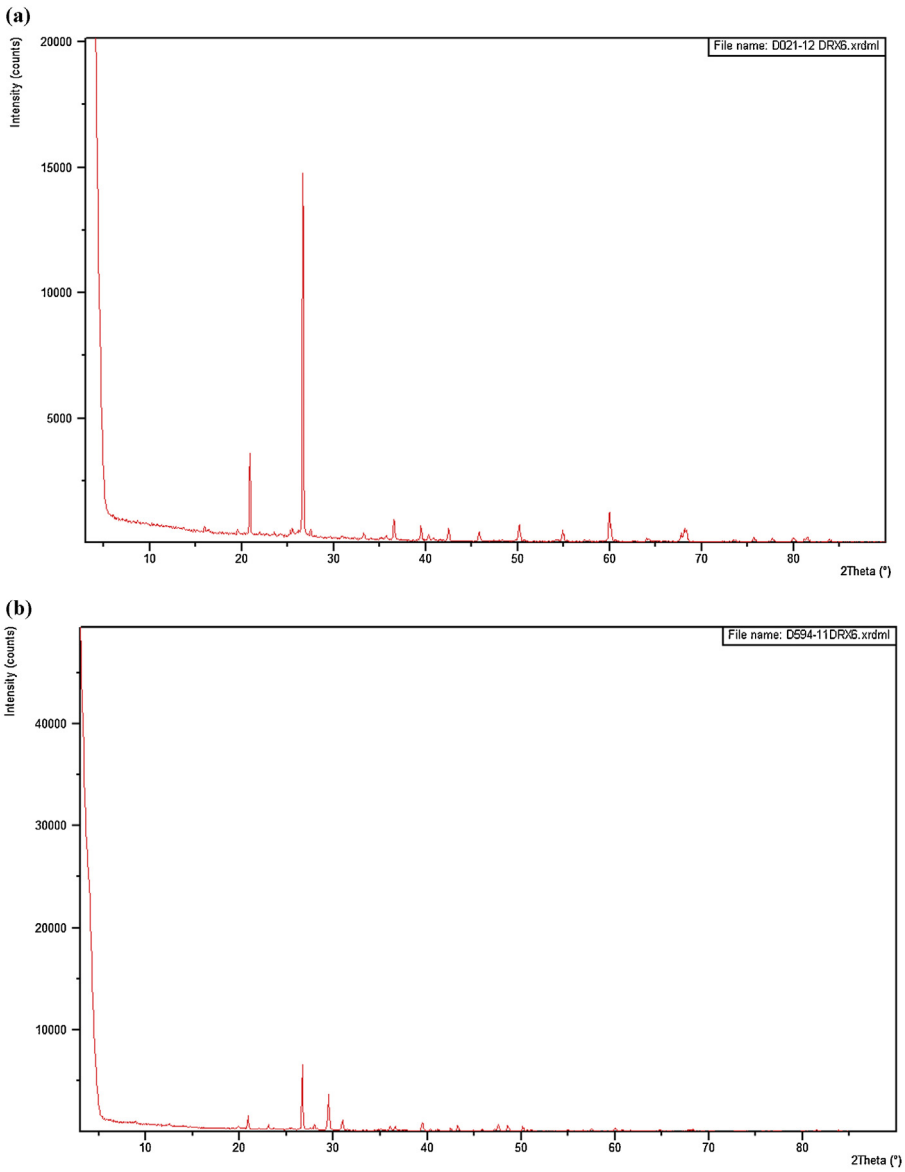

Fig. 2. XRD patterns: (a) magnesite and (b) dolomite.

form of dolomite (double carbonate of calcium and magnesium $(Ca,Mg)(CO_3)_2$). The CaO and MgO contents are 30.4% and 21.7%, respectively. Metals may accompany magnesium and calcium in the structure, and the most common is Fe. Mn, Pb and Zn are often present in trace amounts. The thermal decomposition of dolomite has been widely studied. The decomposition of dolomite in an inert nitrogen (N_2) atmosphere occurs in a single step and can be depicted by the following reaction: $CaMg(CO_3)_2 \rightarrow CaO{\cdot}MgO + 2CO_2$.

Dolomite is presented in solid form recalling the limestone. It is distinguished by the absence of effervescence with dilute hydrochloric acid. It is often grainy and light-colored, but can be powdered. Its density, when it is pure, varies from 2.8 to 2.9 g/cm^3, and its mechanical properties are identical to those of limestone. It does not melt but decomposes from 900 °C losing its CO_2 [2].

Varying amounts of impurities including SiO_2, Al_2O_3 and Fe_2O_3 are present in dolomite. The amounts and types of these impurities may have a large effect on the extent of densification. Dolomite was traditionally used as fettling material for the hearth of furnaces. Dolomites are, as magnesite, used as refractories bricks after being subjected to calcination and sintering at 1600–1700 °C. Dolomite bricks are used in basic soil converters (electric furnaces). Their disadvantage is to present an irregular expansion curve, related to calcium flux content. Dolomite is also used in the glass; it increases the weather resistance of the glass and prevents devitrification. Dolomite is also used as a flux in the manufacture of steel. Dolomite is harder than limestone; it is an excellent building material and can enter in the manufacture of concrete and reconstituted products [2].

The chemical composition of natural dolomite of Morocco is as follows: 36.11% $MgCO_3$ and 57.80% $CaCO_3$. Result indicates that the Moroccan dolomite is relatively pure with an impurity content of around 4.58 wt.%. The mineralogical composition of the two raw materials (magnesite and dolomite) was analyzed using X-ray diffractometer (XPERT DATACOLLECTER software) operating at 40 kV and 40 mA and using CuKα radiation (Fig. 2). The magnesite rock is mainly composed of magnesite mineral, in addition to a small amount of dolomite [2θ: 33.5; 40.5; 50] and quartz [2θ: 26.5]. The dolomitic rock is characterized by the presence of appreciable amount of antigorite mineral [2θ: 23.5], calcite [2θ: 29.5], quartz [2θ: 26.5], and pyrite [2θ: 50.5] beside the major dolomite mineral.

Table 1
Room temperature properties of samples sintered at 1300 °C.

	Total shrinkage (%)	Porosity (%)	Water absorption (%)	Apparent density (g/cm^3)
Magnesite rock	12.3	21.5	14.4	2.1
Dolomite rock	4.1	13.4	5.9	2.6

The fired properties of the samples were evaluated and are given in Table 1. The apparent density, water absorption and open porosity were measured according to ASTMC373-88 [13–15].

3. Process routes

Several efforts have been made by various researchers to improve the high temperature properties of magnesite and dolomite by engineering the microstructure like modification of the grain morphology, amount and distribution of low melting phases and also by changing the chemical and physical nature of bonds. It is evident from a literature survey of about 120 recently published papers that the basic bricks can be used in many industrial applications requiring temperatures greater than 1500 °C. Table 2 summarizes the process conditions, the synthesis/firing temperatures and the characterization of the elaborated basic refractory of various research teams.

4. Magnesia ceramics

Magnesite refractory exhibits various advantageous high temperature properties like high-softening point and excellent chemical endurability in basic condition, and thus the demand for this material has been significantly increased for high temperature applications over the years. Magnesite refractories are widely used in ferrous, non-ferrous and cement industries. They have been extensively used in the steel converter, electric arc furnace and ladle lining in steel-making processes [2]. The primary source for magnesia is natural magnesite along with sea water and inland brine containing the soluble compound magnesium chloride ($MgCl_2$); these final products are referred to as synthetic magnesia. A secondary source of magnesium oxide is from the mining and sintering of brucite deposits; this mineral is composed of magnesium hydroxide ($Mg(OH)_2$) and has a theoretical MgO of about 70 wt.%.

A magnesia refractory is defined by the American Society for Testing and Materials (ASTM) as "a dead-burned refractory material consisting predominantly of crystalline magnesium oxide (MgO)". Also, ASTM defines basic refractories as "refractories whose major constituent is lime, magnesia, or both, and which may react chemically with acid refractories, acid slags, or acidic fluxes at high temperatures". Basic refractories exhibit excellent chemical resistance to other basic refractories, basic slags, or basic fluxes at high temperatures. Magnesium oxide has a very high melting point of about 2800 °C. This characteristic, together with its resistance to basic slags, ubiquitousness, and moderate cost, makes magnesium oxide products the choice for heat-intensive, metallurgical processes such as for the production of metals, cements, and glasses.

As mentioned in the introduction, a chemical analysis of a magnesite will yield the following principal impurities: SiO_2 (silica); CaO (lime); Al_2O_3 (alumina); Fe_2O_3 (iron oxide); and B_2O_3 (boric oxide). These impurities combine together and/or with MgO to form minerals that, under equilibrium conditions, can be predicted from phase equilibrium relationships in the MgO–CaO–SiO_2–Al_2O_3–FeO–Fe_2O_3 system and generally confirmed by X-ray diffraction analyses. Some incorporate suitable additives, which can react with these impurities, convert them into some other high melting phases and thus minimize the amount of low melting phases.

It was reported that TiO_2 reduces the formation of low melting phases [100]. Compacted green pellets and bars of magnesite containing 0–5 wt.% TiO_2 were sintered in the temperature range of 1500–1600 °C with 2 h soaking at peak temperature. It was observed that TiO_2 slightly increased the apparent porosity and decreased the bulk density by reducing the formation of low melting phases. High temperature flexural strength increases with TiO_2 content up to 3 wt.% followed by slight decrease in strength after further increase in the amount of additive. The microstructure of magnesia–zirconia refractories has been studied [112]. It was observed that addition of ZrO_2 reduces the formation of low melting CMS at higher temperature and improves the flexural strength at 1200 °C. Periclase grain shape also changed from rounded to subrounded in the presence of zirconia.

Preparation and characterization of porous MgO–Al_2O_3 refractory aggregates from magnesite and $Al(OH)_3$ as starting raw materials were studied by Yan et al. [106]. The results showed that the Al_2O_3 contents in the porous refractory aggregates strongly affected the spinel formation, change of the neck bonds between the particles, pore structure (porosity, average pore size and pore size distributions), and then affected the strengths. The porous MgO–Al_2O_3 refractory aggregates of 62–72 wt.% Al_2O_3 showed the best combination of high apparent porosities of 42.1–44.2%, high compressive strengths of 51.1–52.0 MPa, high flexural strengths of 17.7–18.6 MPa and small average pore size of 10.81–12.07 μm.

Porous magnesium aluminate spinel ($MgAl_2O_4$) ceramic supports were fabricated by reactive sintering from low-cost bauxite and magnesite at different temperatures ranging from 1100 to 1400 °C and their sintering behavior and phase evolution were evaluated [107]. The supports prepared at 1300 °C showed a homogeneous pore structure, exhibited high flexural strength and excellent chemical resistance.

Other researchers [103] have used hydromagnesite (basic magnesia carbonate) and fumed silica to produce forsterite via solid-state reaction. Liu et al. [79] have studied the thermal decomposition kinetics of magnesite from thermogravimetric data. Thomaidis and Kostakis [108] have prepared cordieritic materials using raw kaolin, bauxite, serpentinite/olivinite and magnesite. The ceramic materials resulted after firing were investigated regarding their phases composition and physical properties of technological interest. By this way, the creation of materials having interesting combinations of properties such as shrinkage, porosity, density, sufficient compressive strength and low coefficient of expansion at high temperatures was achieved. Processing of cordierite-based ceramics from alkaline-earth aluminosilicate glass, kaolin, alumina and magnesite was studied by Tulyaganov et al. [30]. Microstructural changes, porosity evolution and properties of cordierite-based composites have been studied as a function of cordierite–anorthite ratio in modeled ceramic systems. The model systems were composed of alkaline-earth-aluminosilicate glass powder, kaolin, alumina and magnesite. Suitable densification levels of investigated compositions are attained in a narrow temperature range and relatively high residual porosity levels are observed. These features were attributed to the role of the liquid phase during high temperature sintering. Cordierite, anorthite or mixtures of each with mullite are the formed crystalline phases when maximum densification levels are achieved. Their properties are correlated to the processing route and to the composition of sintered materials.

Table 2
Table comparing various research works published between 2000 and 2016.

Research team	Year of publication	Title of paper	General characterization
Gal'yanov et al. [16]	2000	Preparation of magnesite ore in mining	It is shown that the chemical composition of the mined magnesite ore is interrelated with its lumpiness. The results have made it possible to use the effect of segregation for primary preparation of the ore in the mining stage.
Alvarado et al. [17]	2000	Preparation and characterization of MgO powders obtained from different magnesium salts and the mineral dolomite	The decomposition of the precipitated $Mg(OH)_2$ was analyzed by DTA/TGA and XRD. The variation of the properties with the nature of the precursors at 960 °C was studied. The microstructural differences between the MgO agglomerates were examined by SEM at different temperatures.
Warren [18]	2000	Dolomite: occurrence, evolution and economically important associations	Dolomite is not a simple mineral. Dolomite is a metastable mineral, early formed crystals can be replaced by later more stable phases with such replacements repeated a number of times during burial and metamorphism.
Tsirambides [19]	2001	Industrial applications of the dolomite from Potamia, Thassos Island, N. Aegean Sea, Greece	The authors present a detailed characterization and applications of the used dolomite.
Shatilov et al. [20]	2001	A study of the kinetics of decarbonization of magnesite concentrated by flotation	The kinetics of decarbonization of magnesite concentrated by the method of flotation is studied under various conditions (stationary unblown layer, fluidized layer, and layer mixed in a rotary furnace). Typical features of the process of decarbonization of magnesite are determined.
Gropyanov and Gropyanov [21]	2001	Sintering kinetics of MgO studied on magnesite of provenance from the Chita Deposit	An equation is derived that provides an adequate description of the kinetic features of MgO sintering.
Kashcheev [22]	2001	Ways toward improving the technology of refractories based on powdered periclase	A way toward obtaining high-quality powers involves reducing the concentration of SiO_2 in magnesite to 0.2–0.5% and increasing the calcination temperature to 2000–2100 °C to prepare coarse-grained periclase with a crystal size larger than 140 μm.
Samtani et al. [23]	2001	Thermal analysis of ground dolomite, confirmation of results using an X-ray powder diffraction methodology	To investigate if grinding had detrimental effects, a detailed study was carried out using dolomite as the material to be ground.
Zawrah [24]	2001	Characterization and sinterability of chemically precipitated phosphate-bearing magnesia grains	The precipitated powders were characterized for their chemical and mineralogical compositions, thermal analyses and particle size distribution as well as particle morphology. The effect of P_2O_5 was discussed.
Khalil et al. [25]	2001	Aluminous cements containing magnesium aluminate spinel from Egyptian dolomite	The results indicated that the mineralogical compositions were refractory MA spinel, in addition to CA and/or CA_2 phases depending on the composition of the starting materials.
Darweesh [26]	2001	Building materials from siliceous clay and low-grade dolomite rocks	Results showed that the thermal interaction between the constituents of clay and dolomite at 750 °C ensures better and relatively high mechanical strength for the resulting products. The XRD and DTA analyses indicated that the produced articles are composed mainly of carbonates and new formations of calcium silicates, calcium aluminates and MgO in amorphous or fine crystalline state. The fired products after hydraulic hardening at a dried environment recorded the highest mechanical properties.
Sato and Katsura [27]	2001	Experimental investigation on dolomite dissociation into aragonite + magnesite up to 8.5 GPa	This study suggests that the equilibrium line of the dolomite = aragonite + magnesite reaction could be very useful in addition to phase transformation of quartz–coesite and graphite–diamond to constrain *P–T* conditions for the metamorphism of dolomite-bearing ultrahigh-pressure rocks.
Samtani et al. [28]	2001	Isolation and identification of the intermediate and final products in the thermal decomposition of dolomite in an atmosphere of carbon dioxide	The intermediate products were found to be dolomite, calcite and periclase, while the final products were calcium oxide and periclase. Using these results a mechanism of thermal decomposition for dolomite is proposed.
Cunha-Duncan and Bradt [29]	2002	Synthesis of magnesium aluminate spinels from bauxites and magnesias	Four different alumina sources and four different magnesia sources were investigated. The periclase reacts with the free corundum of the bauxite to produce Mg–Al spinel. The periclase then reacts with the mullite in the bauxites to yield additional spinel and also some forsterite.
Tulyaganov et al. [30]	2002	Processing of cordierite-based ceramics from alkaline-earth-aluminosilicate glass, kaolin, alumina and magnesite	Control of the porous structure through manipulation of heating rate was found feasible and easy to implement.
Kalpakli et al. [31]	2002	Effect of binder type and other parameters in synthesis of magnesite chromite refractories from process waste	The optimum sintering temperature was found at 1750 °C.
Serry et al. [32]	2002	Characterization of Egyptian dolomitic magnesite deposits for the refractories industry	XRD, SEM, DTA, DTG, TG and wet chemical analysis methods were applied. According to the research output, pure magnesites with the addition of MgO and/or Fe_2O_3-rich materials are recommended for the production of unshaped MgO–CaO refractories.

Table 2 (*Continued*)

Research team	Year of publication	Title of paper	General characterization
Mustafa et al. [33]	2002	Sintering and microstructure of spinel–forsterite bodies	The spinel–forsterite phase mixtures formed by the addition of different proportions of alumina to forsterite grog's mixes, showed a good compromise of high-density, cold crushing strength and microstructure after firing at 1450 and 1500 °C. Forsterite was first prepared from talc and calcined magnesite at 1400 °C/2 h.
Samtani et al. [34]	2002	Comparison of dolomite decomposition kinetics with related carbonates and the effect of procedural variables on its kinetic parameters	The thermal behavior and the kinetics of decomposition were studied using the Arrhenius equation applied to solid-state reactions. It was found that calcite and dolomite supposedly decompose via a zero-order mechanism while magnesite decomposes via a first-order process.
Kashcheev et al. [35]	2003	Synthesis of spinel from caustic magnesite and alumina dust	The sintering of a mixture of a caustic dust and an alumina dust collected from electric filters taken in MgO/Al_2O_3 ratios of 0.1, 0.28, 0.5, and 0.75 at 1650 °C is studied. Materials with superior physicomechanical properties are obtained: open porosity, 1.2–8.4%; density, 3.5 g/cm^3, and compressive strength, 160–410 MPa. High-density pellets (free of additions) are prepared at a MgO/Al_2O_3 ratio of 0.75, with compressive strength as high as 160 MPa.
Demir et al. [36]	2003	Calcination kinetic of magnesite from thermogravimetric data	It was observed that the process fitted a first-order kinetic model and the values of the activation energies decreased with decreasing particle size, which can be attributed to the increasing particle internal resistance to the escape of CO_2 as the grain size increased.
Beruto et al. [37]	2003	Solid products and rate-limiting step in the thermal half decomposition of natural dolomite in a CO_2(g) atmosphere	Natural dolomite powders obtained from caves, which give unusual high-resistance building materials, have been decomposed in a Knudsen cell at high CO_2 pressures in the temperature range of 913–973 K. XRD traces for the final solid products, after the first half thermal decomposition, have shown that beside the XRD patterns for the calcite and MgO, the existence of a new structure with major peaks at 2θ equal to 38.5° and 65°. This finding has been ascribed to a solid solution of MgO in calcite.
Antonov et al. [38]	2004	Stabilized dolomite refractories	A technology of environment-friendly refractories based on briquetted dry-ground dolomite, magnesia–silicate raw materials, and stabilizing additives has been developed. The potential use of the newly designed refractories as an alternative to chromite–periclase refractories is emphasized.
Serena et al. [39]	2004	Corrosion behavior of $MgO/CaZrO_3$ refractory matrix by clinker	The attack mechanism to substrates of 80% MgO and 20% $CaZrO_3$ (wt.%) obtained from dolomite and ZrO_2 mixtures and MgO and presintetized $CaZrO_3$ mixtures is established.
Yeprem et al. [40]	2004	A quantitative-metallographic study of the sintering behavior of dolomite	Grain growth of the MgO phase during sintering of natural dolomite was studied. For comparison purposes, iron oxide (98.66% mill scale) was added up to 1.5%. The compositions of the phases formed during sintering were studied using XRD and SEM.
Haldar et al. [41]	2004	Effect of compositional variation on the synthesis of magnesite–chrome composite refractory	Magnesite–chrome composites have been prepared by utilizing sintered magnesite and friable chrome ore in presence of titania as additive. The physical properties as well as thermomechanical properties and microstructural studies of the sintered aggregates have been evaluated.
Chen and Tao [42]	2004	Effect of solution chemistry on flotability of magnesite and dolomite	The present study was undertaken to investigate effects of dissolution rate, species distribution, solubility, surface conversion phenomenon, and surface electrical properties on flotability of magnesite and dolomite.
Suvorov et al. [43]	2005	A high-density water-resistant magnesia-lime material based on dolomite	A method for preparation of water-resistant magnesia-lime granules of high density (95–98%) is developed using dolomites and dolomitized magnesites. The use of granulated materials for manufacture of water-resistant clinker, powders, and magnesia-lime refractories with superior performance and economical characteristics is discussed.
Aksel et al. [44]	2005	Investigation of parameters affecting grain growth of sintered magnesite refractories	The parameters influencing grain size of sintered magnesite such as temperature, time, cooling rate and various particle size were investigated using different sintering regimes to improve grain growth. The effects of impurities (SiO_2, CaO, Fe_2O_3, and CaO/SiO_2 ratio) on grain growth were also evaluated by EDX analysis.
Kalaitzaki et al. [45]	2005	Hydraulic lime mortars for the restoration of historic masonry in Crete	This study presents the results of the physicochemical characterization of original mortars and plasters and the evaluation of the repair ones prepared with natural hydraulic lime (NHL) as binding material and siliceous sand and crushed brick as aggregates.
Othman and Nour [46]	2005	Recycling of spent magnesite and ZAS bricks for the production of new basic refractories	The results revealed that, the addition of spent ZAS up to 5.0 wt.% to spent magnesite enhanced the physicomechanical, refractory and thermal properties due to the development of highly refractory phases MA spinel and $MgO{\cdot}ZrO_2$ solid solution.
Pokrovsky et al. [47]	2005	Dissolution kinetics of calcite, dolomite and magnesite at 25 °C and 0–50 atm pCO_2	The obtained results demonstrate that carbonate mineral dissolution rates are not proportional to H_2CO_3(aq) and depend only weakly on pCO_2. For dolomite and magnesite, the surface complexation model (SCM) predicts dissolution rates up to 50 atm pCO_2 with a good accuracy.

Table 2 (*Continued*)

Research team	Year of publication	Title of paper	General characterization
Diaz et al. [48]	2005	Alumina-rich refractory concretes with added spinel, periclase and dolomite: a comparative study of their microstructural evolution with temperature	The evolution of the phases and microstructure was studied as a function of T°C and the processing route for both refractory concretes and their corresponding matrices (<125 μm).
Lingling and Min [49]	2005	Dolomite used as raw material to produce MgO-based expansive agent	The expansion of pastes depends on the making condition and dosage of MgO-based expansive agents greatly. MgO particles burned at lower temperature are bigger than those at high temperature, and resulting in expansion at early age.
Shchekina et al. [50]	2006	Use of magnesian–dolomite mixtures in steel-melting furnace hearths and the mechanism of their wear in service. 1. Study of hearth refractory mixture	The results of mineralogical-petrographic analysis of magnesian–dolomite refractory mixture used in the hearths of steel-melting furnaces are described. The variation regularities of its phase and chemical composition are identified and the mechanism of its wear in service at the metallurgical works in is considered.
Solodkii and Shamrikov [51]	2006	The ural mineral raw-material base for the ceramics, refractory, and glass industry	Brief information is reported on the promising deposits of clays and kaolins, feldspars and their substituents, quartz minerals, carbonate rocks, pyrophyllites and kyanites, magnesia and magnesia–silicate materials, and many other types of raw materials for the ceramics, glass, and refractories industry.
Ye and Troczynski [52]	2006	Hydration of hydratable alumina in the presence of various forms of MgO	The results revealed significant difference in the hydration products between the hydratable alumina-reactive magnesia mixture and the hydratable alumina-fused magnesite or dead burnt magnesite mixtures under the hydration conditions.
Kangal and Guney [53]	2006	A new industrial mineral: huntite and its recovery	Characterization of huntite ores was made and separation conditions for huntite from the associated mineral, magnesite were investigated.
Gonzalez et al. [54]	2007	Copper matte penetration resistance of basic refractories	The effects of oxygen potential and matte grade on burned magnesite–chrome brick and spinel direct-bonded brick were studied using operating conditions typical of copper converters, and their relative performance was evaluated using high-grade and low-grade matte at oxygen potentials of 10^{-7} and 10^{-6} atm.
Ghosh et al. [55]	2007	Effect of MgO and ZrO_2 additions on the properties of magnesite–chrome composite refractory	The reactivity of magnesia was found to play an important role in the final properties of samples. Introducing less reactive sintered magnesia improved all the properties of the aggregates. ZrO_2 was found to be a good sintering aid in the magnesite–chrome composites.
Yeprem [56]	2007	Effect of iron oxide addition on the hydration resistance and bulk density of doloma	According to the results of experiments with 15 sintered samples, sintering temperature, soaking time and increase of mill scale amount were found to increase the bulk density and thus decrease the observed apparent porosity.
Mako [57]	2007	The effect of quartz content on the mechanical activation of dolomite	The increased quartz content accelerated the mechanochemical deformation and amorphization of dolomite phase. After grinding the dolomite/quartz mixtures, the thermal decomposition of dolomite showed a four- or three-step weight loss, instead of the original two- or one-step one.
Diaz and Torrecillas [58]	2007	Phase development and high temperature deformation in high alumina refractory castables with dolomite additions	A correlation between the microstructural phase evolution and the creep behavior with temperature was established.
Kurama et al. [59]	2007	Investigation of borax waste behavior in tile production	The addition of TSW appeared to improve liquid phase development with better physical properties compared to those of standard composition for the firing regime involved. The results indicated a prospect for using the waste as a co-flux in wall tile formulations.
Kalpakli [60]	2008	Investigation of TiO_2-added refractory brick properties from calcined magnesite raw material	90% magnesite–10% chromite composition was used as a brick composition. Compaction pressure, sintering temperature, ratio of TiO_2 addition, and influence of bonding type on refractory properties were examined. Experiments show that using a magnesite particle size of -10^{-3} m and a chromite particle size of -63×10^{-6} m affects the properties of the product in a positive way.
Diaz et al. [61]	2008	Room temperature mechanical properties of high alumina refractory castables with spinel, periclase and dolomite additions	From room temperature to 1000 °C the refractory castables present a pronounced non-linear stress–strain behavior both in the uniaxial tensile and compressive modes, as a result of damage to the microcrack network. Above 1000 °C the refractory castables begin to sinter owing to a transitory liquid phase, the crystallization of calcium aluminate cement phases and the self-forming spinel phase.
Peiwei et al. [62]	2008	Using a new composite expansive material to decrease deformation and fracture of concrete	Using minerals of dolomite, serpentine and magnesite produce a new composite material, which provides an expansive stress to decrease deformation and fracture of hydraulic concrete.
Aksel'rod et al. [63]	2008	Refractory materials and methods for increasing the life of converter linings from experience of OOO Gruppa Magnezit	Experience of using Gruppa Magnezit refractory materials in the lining of acid converters in Russia and the Ukraine is summarized briefly.

Table 2 (*Continued*)

Research team	Year of publication	Title of paper	General characterization
Prokof'ev et al. [64]	2009	Physical–chemical phenomena occurring during the production of sorbent from a clay–dolomite composition	It is shown that kaolinite plays a decisive role in the formation of the porous structure of granules and dolomite determines the strength of the articles produced.
Rabah and Ewais [65]	2009	Multi-impregnating pitch-bonded Egyptian dolomite refractory brick for application in ladle furnaces	Dolomite brick samples containing 10 wt.% coal tar pitch and pressed at 108 MPa have high hydration resistance compared to the hydration resistance of the commercial. The prepared brick samples have acceptable density, chemical stability, outstanding resistance and good mechanical properties would meet the requirements of ladle furnace (LF) for steel-making industry.
Siadati and Monshi [66]	2009	Acidic and basic binders for magnesite-based aggregate in plaster of tundish	Cold crushing strength at different heat treatments is measured. Apparent porosity of samples without pulp and bulk density together with pH of the binder solution is evaluated and XRD and SEM studies are performed.
Martinez et al. [67]	2009	Sintering behavior of periclase–doloma refractory mixes	The analyzed mixes mainly contain periclase and doloma, with iron oxides. Sintering began at temperatures higher than 1200 °C and was associated to liquid phase formation.
Adriano et al. [68]	2009	Microscopic characterization of old mortars from the Santa Maria Church in Évora	The characterization methodology involved a multidisciplinary set of chemical, physical, microstructural and mechanical techniques, and gave special attention to the use of microstructural characterization techniques, particularly petrographical analysis and SEM for the identification of the mortar's constituents as well as in the evaluation of the state of conservation.
Das et al. [69]	2010	Microstructural and densification study of natural Indian magnesite in presence of zirconia additive	The sintering and microstructural evaluation of magnesite was carried out in presence of zirconia. A crystalline phase, magnesio–zirconate, was identified at the triple point regions of the direct-bonded periclase grains.
Yamamoto et al. [70]	2010	Antibacterial characteristics of $CaCO_3$–MgO composites	Composite powders contributing to oral hygiene application, i.e. nano-scale MgO crystallite dispersed in $CaCO_3$ grain, were fabricated by the thermal decomposition of dolomite.
Szczerba and Pędzich [71]	2010	The effect of natural dolomite admixtures on calcium zirconate–periclase materials microstructure evolution	The material obtained from the mixture of zirconium oxide and natural dolomite with the high impurities content has the highest densification level at 1500 and 1600 °C.
Mahadi and Palaniandy [72]	2010	Mechanochemical effect of dolomitic talc during fine grinding process in mortar grinder	Dolomitic talc was milled in a mortar mill by varying the milling time, solid content, and vertical stress. The milled samples exhibited massive particle size reduction and came to a threshold value around 4 μm, with wider particle size distribution.
Hojamberdiev et al. [73]	2010	Characterization and processing of talc-magnesite from the Zinelbulak deposit	Petrographic analysis confirmed the presence of magnesite and breunnerite. The dressability of the Zinelbulak talc-magnesite was tested using conventional gravity concentration, flotation and electromagnetic separation. Subsequent flotation and magnetic separation techniques could further increase the yield of high-quality magnesite and talc. Refractory samples prepared by heating the separated magnesite at 1600 °C for 2 h met the State Standards for refractory materials.
Hojamberdiev et al. [74]	2011	Processing of refractory materials using various magnesium sources derived from Zinelbulak talc-magnesite	A series of refractory materials were prepared on the basis of these magnesium sources, and their effects on physicomechanical properties and microstructures were investigated as a function of sintering temperature, molding pressure, and the particle size of magnesium sources.
Khater [75]	2011	Influence of Cr_2O_3, LiF, CaF_2 and TiO_2 nucleants on the crystallization behavior and microstructure of glass-ceramics based on blast-furnace slag	Glass-ceramics based on blast-furnace slag (56.78 wt.%) were prepared by mixing quartz sand, dolomite, limestone, and clay as other batch constituents.
Obregón et al. [76]	2011	MgO–$CaZrO_3$-based refractories for cement kilns	Two series of refractory materials have been designed taking into account the phase equilibrium relationships to obtain MgO–$CaZrO_3$–Ca_2SiO_4–$Ca_3Mg(SiO_4)_2$ or MgO–$CaZrO_3$–$Ca_3Mg(SiO_4)_2$–c-ZrO_2 as final crystalline phases. Specimens have been fabricated by reaction sintering of natural dolomite and zircon and with dead burned magnesia aggregates. Different relationships between the proportion and sizes of the fines and the aggregates have been explored.
Khater and Morsi [77]	2011	Glass-ceramics based on spodumene–enstatite system from natural raw materials	Glasses of compositions (wt.%) corresponding to 50–90 spodumene and 50–10 enstatite were prepared depending on natural raw materials and Li_2CO_3 as small ingredient. The crystallization behavior was studied using DTA and XRD. The effect of addition of the nucleating agents (LiF) to a selected glass was also examined.
Urvantsev and Kashcheev [78]	2012	Magnesite enrichment by a dry method	Results are provided for enrichment of low-grade magnesite deposit (MgO 43.1%) by electric separation.

Table 2 (*Continued*)

Research team	Year of publication	Title of paper	General characterization
Liu et al. [79]	2012	Thermal decomposition kinetics of magnesite from thermogravimetric data	Thermal decomposition kinetics of magnesite were investigated using non-isothermal TG-DSC technique at heating rate (β) of 15, 20, 25, 35, and 40 K min^{-1}. A new multiple rate iso-temperature method was used to determine the magnesite thermal decomposition mechanism function, based on the assumption of a series of mechanism functions.
Ghosh and Tripathi [80]	2012	Sintering behavior and hydration resistance of reactive dolomite	Sintering of raw dolomite and hydroxides derived from dolomite was carried out in the temperature range 1350–1650 °C. Hydration resistance was related to densification and grain size of sintered dolomite.
Dwarapudi et al. [81]	2012	Effect of MgO in the form of magnesite on the quality and microstructure of hematite pellets	it was observed that with increasing MgO, swelling characteristics of pellets were found to be improved. Reducibility of the pellets improved substantially in the range of 0.5–1.5% MgO. Formation of magnesioferrite phase and high melting point slag formed during induration could be attributed to the improved quality of pellets.
Lampropoulou et al. [82]	2013	New periclase-spinel refractories from densely sintered high-purity magnesite and new synthetic compositions based on spinel. Part 1. Study of mineral composition, microstructure, thermal expansion, and ultimate strength in compression	Sintered magnesite and synthesized spinel properties are provided. On the basis of petrographic criteria, and also linear thermal expansion coefficient (LTEC) and ultimate strength in compression for final materials, the authors of this article propose a most suitable material with respect to quality for testing in high temperature branches of industry.
Cho et al. [83]	2013	Air gasification of mixed plastic wastes using calcined dolomite and activated carbon in a two-stage gasifier to reduce tar	Stable gasification of mixed plastic wastes was conducted in a two-stage gasifier. Strong tar removal was achieved with the combination of activated carbon and dolomite. Increasing amount of activated carbon resulted in less tar and high hydrogen production. Chlorine in feed material was mainly transferred to char or captured by activated carbon.
Macris et al. [84]	2013	Experimental determination of equilibrium magnesium isotope fractionation between spinel, forsterite, and magnesite from 600 to 800 °C	The authors performed experiments at 600, 700, and 800 °C and 1 GPa to establish the equilibrium magnesium isotope partitioning between forsterite (Mg_2SiO_4) and magnesite ($MgCO_3$) and between spinel ($MgAl_2O_4$) and magnesite, making use of the carbonate as an isotope exchange medium to overcome sluggish diffusion-limited magnesium isotope exchange between spinel and forsterite.
Othman [85]	2013	Effect of talc and bauxite on sintering, microstructure, and refractory properties of Egyptian dolomitic magnesite	Mineralogical composition and microstructure, pore size distribution, and mechanical and refractory properties of samples were investigated. Most samples showed high refractoriness under load, good spalling resistance, better mechanical properties than current refractories, and compact microstructure.
Sasaki et al. [86]	2013	Effect of natural dolomite calcination temperature on sorption of borate onto calcined products	The sorption density of borate was greater with the calcined products at 700 °C than 800–900 °C and under an Ar gas flow system rather than for static air at the same temperatures. The surface reactivity of the calcined dolomite with borate in the aqueous phase was affected by CO_2 emitted in the decarbonation at higher temperatures.
Wang et al. [87]	2013	New synthetic route to Mg–Al–CO_3 layered double hydroxide using magnesite	The crystal morphology of the prepared LDH displays platelet-like structure with a hexagonal shape, which is agreed with the LDH produced by industrial chemicals. Thermal analysis indicated that the total weight loss was 43.8% in the range of 20–850 °C.
Tian et al. [88]	2014	An experimental study on thermal decomposition behavior of magnesite	Thermal decomposition of magnesite is investigated by using a TG–MS. Different kinetic methods including Coats–Redfern, Flynn–Wall–Ozawa, and Kissinger–Akahira–Sunose are used to investigate the thermal decomposition kinetics of magnesite. It was observed that the activation energy values obtained by these methods are similar.
Soltan et al. [89]	2014	Densification and resistance to hydration and slag attack of ilmenite-doped MgO-dolomite refractories in relation to their thermal equilibrium and microfabric	This work aims at studying rate of densification, resistance to hydration and slag attack of 0.0–2.0 wt.% ilmenite-doped MgO-dolomite refractories fired at 1400–1700 °C, in relation to their thermal equilibrium and microfabric. XRF, XRD, SEM, EDAX and mercury intrusion were used to characterize the fired samples.
Charalampides et al. [90]	2014	The contribution of industrial minerals to sustainable recovery of Greek Economy	Occurrences and industrial mineral deposits, primarily in North Greece, are examined in relation to their uses, such as feldspars, pozzolan, pumice, kaolin, zeolites, quartz, gypsum, and white carbonates.
Fu et al. [91]	2014	Kinetics of extracting magnesium from mixture of calcined magnesite and calcined dolomite by vacuum aluminothermic reduction	The results indicate that the reduction rate is increased with increasing temperature, content of aluminum and pellet forming pressure. The XRD patterns confirm that the reduction process can be roughly classified into three stages: the formation of $MgAl_2O_4$, and $Ca_{12}Al_{14}O_{33}$ phases; the phase transformation from $MgAl_2O_4$ and $C_{12}A_7$ to $CaAl_2O_4$; the formation of $CaAl_4O_7$ phase.
Gao et al. [92]	2014	Characteristics of calcined magnesite and its application in oxidized pellet production	Experimental resulting indicated that the best calcination condition was 850 °C and 1 h. Under this condition, the hydration activity of the calcined magnesite was 88.56%.

Table 2 (*Continued*)

Research team	Year of publication	Title of paper	General characterization
Valle-Zermeno [93]	2014	Reutilization of low-grade magnesium oxides for flue gas desulfurization during calcination of natural magnesite: a closed-loop process	Three different by-products from the calcination of natural magnesite were selected in order to evaluate their desulfurization capacity.
Huang et al. [94]	2014	Effects of calcite and magnesite application to a declining Masson pine forest on strongly acidified soil in Southwestern China	Both calcite and magnesite additions caused a significant increase in pH and a decrease in dissolved inorganic monomeric aluminum concentration of soil water. Calcite addition may further decrease the Mg^{2+} availability in soil water, thereby exacerbating Mg^{2+} deficiency in the acidified forest soils of southern and southwestern China.
Fu et al. [95]	2014	Mechanism of extracting magenesium from mixture of calcined magnesite and calcined dolomite by vacuum aluminothermic reduction	The first stage included the direct reaction between calcined dolomite or calcined magnesite and Al with $12CaO{\cdot}7Al_2O_3$ and $MgO{\cdot}Al_2O_3$ as products. The CA phase was mainly produced in the second stage and the overall reaction rate was determined by both the diffusion of Ca^{2+} with molten Al and the chemical reaction. The CA_2 phase was mainly produced in the third stage and the reaction process was controlled by the diffusion of Ca^{2+}.
Ghosh et al. [96]	2014	Studies on densification, mechanical, microstructural and structure–properties relationship of refractory aggregates prepared from Indian magnesite by changing lime–silica ratio	The sintered material has been characterized in terms of bulk density, apparent porosity, true density, relative density, cold modulus of rupture, hot modulus of rupture, thermal shock resistance, structural properties by XRD in terms of phase identification and evaluation of crystal structure parameters of corresponding phases by Rietveld analysis.
Gadikota et al. [97]	2014	Morphological changes during enhanced carbonation of asbestos containing material and its comparison to magnesium silicate minerals	Formation of phases such as dolomite ($(Ca, Mg)(CO_3)_2$), whewellite ($CaC_2O_4{\cdot}H_2O$) and glushinskite ($MgC_2O_4{\cdot}2H_2O$) and a reduction in the chrysotile content was noted.
Zhang et al. [98]	2014	Reaction kinetics of dolomite and portlandite	Pressed pellets of dolomite develop calcite at both exterior surfaces and in the interior, where calcite develops as a secondary phase but is not morphologically well-formed crystals.
Liu et al. [99]	2015	Experimental investigation on the properties and microstructure of magnesium oxychloride cement prepared with caustic magnesite and dolomite	The results indicated that MOCs (magnesium oxychloride cements) prepared with caustic magnesite and dolomite obtained a good engineering performance.
Kumar et al. [100]	2015	Effect of titania on the microstructure evolution of sintered magnesite in correlation with its properties	It was observed that TiO_2 slightly increased the apparent porosity and decreased the bulk density by reducing the formation of low melting phases.
Lavat et al. [101]	2015	The firing steps and phases formed in Mg–Zr–Al refractory dolomite-based materials	This study was carried out in order to determine the feasibility of using Argentine dolomites in the preparation of $CaZrO_3$–$MgAl_2O_4$ by solid-state reaction. The thermal and structural changes which occur during the firing of the batches up to 1425 °C were studied by the combination of diffractometric and infrared spectroscopic data at the most remarkable reaction steps. The final product is composed mainly by $MgAl_2O_4$, $CaZrO_3$, and Ca_2SiO_4 phases and the optimal synthesis temperature would be 1425 °C.
Kıpçak and Isıyel [102]	2015	Magnesite tailing as low-cost adsorbent for the removal of copper(II) ions from aqueous solution	The removal of Cu(II) ions from aqueous solution using magnesite tailing was investigated. Batch kinetic and equilibrium experiments were conducted to study the effects of initial pH, adsorbent dosage, contact time, initial concentration and temperature. The results showed that magnesite tailing is a suitable adsorbent for the removal of Cu(II) ions from aqueous solutions.
Chen et al. [103]	2015	Low temperature synthesis of forsterite from hydromagnesite and fumed silica mixture	The phase development and morphology evolution of the hydromagnesite and hydromagnesite–fumed silica mixture during heat treatment were characterized by SEM, BET nitrogen-gas adsorption method, and XRD. Monolithic forsterite was synthesized after calcination of the hydromagnesite–fumed silica mixture at 1100 °C.
Wang et al. [104]	2015	Role of $Mg_xCa_{1-x}CO_3$ on the physical–chemical properties and cyclic CO_2 capture performance of dolomite by two-step calcination	Two-step calcination treated dolomite sorbent was prepared and characterized. An intermediate phase ($Mg_xCa_{1-x}CO_3$) was observed by TG and XRD results.
Chen et al. [105]	2015	Influence of MgO precursors on mechanically activated forsterite synthesis	Brucite-fumed silica and hydromagnesite-fumed silica mixtures were used to investigate the influence of MgO precursors on mechanically activated forsterite synthesis. The changes in morphology, chemical bond and phase composition of the ground and calcined mixtures were examined with SEM, XPS and XRD.
Yan et al. [106]	2015	Preparation and characterization of porous MgO–Al_2O_3 refractory aggregates using an in situ decomposition pore-forming technique	The porous MgO–Al_2O_3 refractory containing 30–92 wt.% Al_2O_3 were prepared via an in situ decomposition pore-forming route using magnesite and $Al(OH)_3$. The results showed that the Al_2O_3 contents in the porous refractory aggregates strongly affected the spinel formation, change of the neck bonds between the particles, pore structure and then affected the strengths.

Table 2 (*Continued*)

Research team	Year of publication	Title of paper	General characterization
Wang et al. [107]	2015	Preparation and characterization of porous $MgAl_2O_4$ spinel ceramic supports from bauxite and magnesite	The effects of sintering temperature on the pore structure, size and distribution as well as on the main properties of spinel ceramic supports such as flexural strength, nitrogen permeation flux and chemical resistance were investigated.
Thomaidis and Kostakis [108]	2015	Synthesis of cordieritic materials using raw kaolin, bauxite, serpentinite/olivinite and magnesite	The ceramic materials resulted after firing, were investigated regarding their phases composition and physical properties of technological interest.
Albhilil et al. [109]	2015	Thermal and microstructure stability of cordierite–mullite ceramics prepared from natural raw materials – Part II	The refractoriness of samples is found to be higher. XRD shows that heating–quenching procedure has led to crystallization of cordierite and mullite phases.
da Cruz and Bragança [110]	2015	Evaluation of the protective C_2S layer in the corrosion process of doloma-C refractories	C_2S layer samples were characterized by analyzing their chemical composition, phase formation and microstructure.
Temiz et al. [111]	2015	Influence of blast-furnace slag on behavior of dolomite used as a raw material of MgO-type expansive agent	Volume expansion of paste samples increased with increasing dolomite content. However, it decreased with addition of BFS. Length change samples containing dolomite + BFS was less than one containing sole dolomite but more than reference samples.
Burhanuddin et al. [112]	2015	Effect of zirconia on densification and properties of natural Indian magnesite	ZrO_2 was added to reduce the formation of low melting phase in order to improve the hot strength.
Booth et al. [113]	2015	Effect of impurities and sintering temperature on properties of $MgO–CaZrO_3$ ceramics	The influence of the different mineralogy of the dolomites and sintering temperatures on the properties of the composites was investigated. Ceramics had porosity of 20–30%, the representative microstructure as determined using SEM–EDX was constituted by $CaZrO_3$, MgO grains containing some m-ZrO_2 grains.
Raza et al. [114]	2015	Leaching of natural magnesite ore in succinic acid solutions	The results indicated that the extraction of magnesium depends on acidic strength, reaction temperature, ore particle size, stirring rate and liquid solid ratio.
Dębska [115]	2015	The effect of exposition conditions on the durability of cement concrete with dolomite aggregate sourced near Kraków, Poland	The observation of linear extension as well as changes in compressive strength and surface alteration due to corrosive exposition conditions were the key diagnostic features adopted for this examination.
Li et al. [116]	2015	Low temperature synthesis of calcium–hexaluminate/magnesium–aluminum spinel composite ceramics	Calcium–hexaluminate/magnesium–aluminum spinel ceramic composites were synthesized at 1450 °C for 3 h using a precursor from dolomite and industrial aluminum hydroxide through a 200 °C hydrothermal treatment, which was 100 °C lower than the traditional process.
Formosa et al. [117]	2015	Magnesium phosphate cements formulated with a low-grade MgO by-product: physicomechanical and durability aspects	MPC formulated with LG-MgO by-product were selected from preliminary study. Durability studies show good durability and repairing properties.
Sifré et al. [118]	2015	Effects of temperature, pressure and chemical compositions on the electrical conductivity of carbonated melts and its relationship with viscosity	Evidence for a relationship between melt electrical conductivity and melt viscosity. Less than 0.2% of carbonated melt explains electrical conductivity below Brazilian craton.
Xie et al. [119]	2016	The thermochemical activity of dolomite occurred in dolomite–palygorskite	The decomposition temperature of dolomite occurred in DPC started at 500 °C and ended at 780 °C, with a maximum peak at 745 °C. The decomposition temperature of dolomite in DPC was found to be 50 °C lower than that of common dolomite.
Chen et al. [120]	2016	Comparison of the chemical corrosion resistance of magnesia-based refractories by stainless steel-making slags under vacuum conditions	This study evaluates commercially available magnesia–chromite, magnesia–carbon and magnesia–doloma bricks for their use in a vacuum oxygen decarburisation ladle. The corrosion behavior of these bricks by stainless steel-making slags is, therefore, investigated through crucible tests in a vacuum induction furnace at elevated temperatures and low oxygen partial pressures. The results reveal that magnesia–carbon bricks are severely corroded due to the high dissolution of MgO, while magnesia–chromite and magnesia–doloma refractories exhibit an excellent corrosion resistance.
Gautier et al. [121]	2016	Magnesite growth inhibition by organic ligands: an experimental study at 100, 120 and 146 °C	The authors show the influence of three organic ligands: oxalate, citrate and EDTA on magnesite growth in alkaline conditions and at hydrothermal temperatures (100, 120 and 146 °C) using mixed flow reactors.
Masindi and Gitari [122]	2016	Simultaneous removal of metal species from acidic aqueous solutions using cryptocrystalline magnesite/bentonite clay composite: an experimental and modeling approach	The overall aim of the present study was to fabricate cryptocrystalline magnesite and bentonite clay composite and evaluate its application for simultaneous removal of Co(II), Cu(II), Ni(II), Pb(II) and Zn(II) from wastewater in a single step.
Masindi et al. [123]	2016	Synthesis of cryptocrystalline magnesite–bentonite clay composite and its application for neutralization and attenuation of inorganic contaminants in acidic and metalliferous mine drainage	The capacity of the composite to neutralize acidity and remove toxic chemical species from synthetic and field AMD was evaluated at optimized conditions. Interaction of the composite with AMD led to an increase in pH (pH > 11) and lowering of metal concentrations.

Forsterite was prepared from Egyptian talc and calcined magnesite at 1400 °C/2 h [33]. The material shows good density but the microstructure contains cracks along the grain boundaries affecting the mechanical properties. The sintering and mechanical properties are improved through the addition of alumina. Thermal and microstructure stability of cordierite–mullite ceramics prepared from kaolin, magnesite, quartz and $Al(OH)_3$ was studied by Albhilil et al. [109]. X-ray diffraction (XRD), scanning electron microscopy and mercury intrusion porosimetry (MIP) have been used to characterize the samples before and after heating–quenching test. The refractoriness of samples is found to be higher. XRD shows that heating–quenching procedure has led to crystallization of cordierite and mullite phases.

Magnesite–chrome composites have been prepared by utilizing sintered magnesite and friable chrome ore in presence of titania as additive [41]. Three types of batch compositions containing 5% Cr_2O_3, 18% Cr_2O_3 and 30% Cr_2O_3 have been selected for developing mag–chrome composites. The physical properties as well as thermomechanical properties and microstructural studies of the sintered aggregates have been evaluated.

The parameters influencing grain size of sintered magnesite such as temperature, cooling rate and various particle size were investigated by Aksel et al. [44]. For the samples sintered at 1700 °C, the decrease in the cooling rate from 10 to 5 °C min^{-1} and the increase in the dwell time from 19 to 50 min enhanced grain size significantly.

The reutilization of low-grade magnesium oxides for flue gas desulfurization during calcination of natural magnesite was also studied by Zermeño et al. [93]. Magnesium oxychloride cements with different amounts of active magnesium oxide were prepared with caustic magnesite and dolomite [99]. The fluidity, compressive and flexural strength were measured. The results indicated that the prepared materials with caustic magnesite and dolomite obtained a good engineering performance. Siadati and Monshi [66] have studied the effect of nature of binders for magnesite-based aggregates. In their work, sulfate binders, such as sulfamic acid, H_2NSO_3H; aluminum sulfate, $Al_2(SO_4)_3$; ammonium sulfate, $(NH_4)_2SO_4$; magnesium sulfate, $MgSO_4$; calcium sulfate, $CaSO_4$; sodium sulfate, Na_2SO_4; and potassium sulfate, K_2SO_4, are investigated. Cold crushing strength at different heat treatments of room temperature, 110 °C, 1100 °C, and 1400 °C is measured. Apparent porosity of samples without pulp and bulk density together with pH of the binder solution is evaluated and XRD and SEM studies are performed. Among these sulfate binders, $MgSO_4$ was found to be the best. It is acidic in nature and develops strong bonds to the basic aggregate, MgO, at low temperatures. At high temperatures, it dissociates from MgO(s) and SO_3(g) and the remaining portion of MgO is the same as host oxide, with no corrosion and easy deskulling. Basic binders such as calcium sulfate, sodium sulfate and potassium sulfate could not strongly bond the MgO aggregates.

5. Doloma ceramics

The term "doloma" refers to the calcined dolomite. Doloma consists of a phase mixture of lime (CaO) and periclase (MgO). Doloma is the semi-product used to produce dolomite refractory. They have extremely high melting points, as the eutectic for the CaO–MgO binary system occurs at 2370 °C. Doloma is a material that is susceptible to hydration and thus its free lime ratio must be lower than a critical value. A usable doloma should have a bulk density greater than 3 g/cm^3. Varying amounts of other impurities, including SiO_2, Al_2O_3, and Fe_2O_3, are usually present. The amounts and types of the accessory oxides may have a large effect on the extent of densification, as it has been established that with these impurities sintering may occur by a liquid phase mechanism. It has been reported that the trivalent oxides, especially Fe_2O_3, enhance the sintering during the commercial manufacturing process. Doloma is one of the attractive steel-making refractories because of its potential cost effectiveness and worldwide abundance [124].

Doloma is an excellent refractory for use in many steel-making applications since it is thermodynamically stable to slags and metal. The two major constituents of doloma, CaO and MgO, are among the more stable of the refractory oxides [5]. A doloma refractory containing less than 1% SiO_2 is far more thermodynamically stable than high alumina or even magnesite refractories.

Refractory-grade doloma typically contains less than 2.5% impurities (silica, iron oxide, and alumina) and greater than 97.5% CaO + MgO. Most high-purity dolomite deposits are difficult to calcine and sinter to high density and usually require special methods to yield an acceptable refractory-grade doloma. The carbonate (dolomite) is converted to the oxide (doloma) and sintered to the required density in either a rotary kiln or a shaft kiln operating at 1850 °C or greater. There are basically two different production routes: single-pass process and double-pass process [124].

The good slag-resistant characteristics of doloma are a result of the presence of free lime not found in other refractories of lower basicity. In contact with slags not fully saturated with lime, a dense layer of recrystallized lime and dicalcium silicates forms on the hot face of the brick, limiting further slag penetration. Basically, the slag's reaction with the lime stops penetration, slowing down overall wear. However, slags deficient in lime but high in R_2O_3 oxides can be quite aggressive to a doloma brick. This is due to the formation of calcium aluminates and/or ferrites that have melting points significantly below 1600 °C.

Lingling and Min [49] have used dolomite as raw materials to produce MgO-based expansive agent. On the characteristics of decomposition of dolomite, the authors think it is possible to use dolomite as raw material, but the silica-bearing mineral is considered to combine the CaO released from dolomite to form silicate. The phases of MgO-based expansive agent are mainly MgO, C_2S and a little amount of CaO. Yeprem et al. [40] have studied the effect of iron oxide addition on the hydration resistance and bulk density of doloma. The resulting bulk densities and apparent porosities of the sintered doloma are investigated. According to the results of experiments with 15 sintered samples, sintering temperature, soaking time and increase of mill scale amount were found to increase the bulk density and thus decrease the observed apparent porosity. In hydration resistance tests, it seemed that the same characteristics also increased the resistance. Natural dolomite powders obtained from caves, which give unusual high-resistance building materials, have been decomposed at high CO_2 pressures in the temperature range of 1176–1246 °C [37]. XRD traces for the final solid products, after the first half thermal decomposition, have shown that beside the XRD patterns for the calcite and MgO, the existence of a new structure with major peaks at 2θ equal to 38.5° and 65°. This finding has been ascribed to a solid solution of MgO in calcite. Xie et al. [119] have studied the thermochemical activity of dolomite that occurred in dolomite–palygorskite (DP). The phase, microstructure, and morphology of DP were characterized before and after calcination using X-ray diffraction (XRD), field emission scanning electron microscopy (FE-SEM), and transmission electron microscopy (TEM). Additionally, the process of thermal decomposition of DPC was determined by thermal gravity (TG) and differential thermal gravity (DTG) analysis and was compared with that of common dolomite. The results showed that the decomposition temperature of dolomite that occurred in DPC started at 500 °C and ended at 780 °C, with a maximum peak at 745 °C.

Due to the open pore microstructure, MgO–$CaZrO_3$ refractory composites are considered useful materials in various industrial applications. However, the reactivity of the MgO limits its utilization in acid conditions. Lavat et al. [101] have used dolomite in the preparation of $CaZrO_3$–$MgAl_2O_4$ by solid-state reaction. The

thermal and structural changes that occur during the firing of the batches up to 1425 °C were studied by the combination of diffractometric and infrared spectroscopic data at the most remarkable reaction steps. The final product is composed mainly by $MgAl_2O_4$, $CaZrO_3$, and Ca_2SiO_4 phases and the optimal synthesis temperature would be 1425 °C. Tomba Martinez et al. [67] have studied the sintering behavior of periclase–doloma refractory mixes. Results showed that the analyzed mixes mainly contain periclase and doloma, with a wide granulometric distribution and different content of minor components (mainly, iron oxides). Material sintering began at temperatures higher than 1200 °C and was associated to liquid phase formation. Differences in sintering mechanisms with distinct amounts of liquid phase involved were determined in the analyzed materials and related to their iron oxides contents. Well-sintered specimens with higher room temperature mechanical strength and lower porosities were obtained from the mix with highest iron oxide content.

Mixes of calcium aluminate cements containing MA spinel were prepared using appropriate mixtures of Egyptian dolomite (MgO, 20.16% and CaO, 31.32%) with active alumina (99.50%) [25]. The cement mixes were prepared at 1600 °C using the sintering method. The results indicated that their mineralogical compositions were refractory MA spinel, in addition to CA and/or CA_2 phases depending on the composition of the starting materials. The prepared cements exhibited a compromise between considerable strength and higher refractoriness.

Building bricks could be prepared from mixtures of low melting clay and low-grade dolomite rocks after firing at a relatively low firing temperature of 750 °C [26]. Results showed that the thermal interaction between the constituents of clay and dolomite at 750 °C ensures better and relatively high mechanical strength for the resulting products. The XRD and DTA analyses indicated that the produced articles are composed mainly of carbonates and new formations of calcium silicates, calcium aluminates and MgO in amorphous or fine crystalline state. The fired products after hydraulic hardening at a dried environment recorded the highest mechanical properties.

A method of preparation of multi-impregnated pitch-bonded dolomite refractory brick for ladle furnace was described by Rabah and Ewais [65]. Brick samples were prepared from blend of calcined dolomite mineral and coal tar pitch. The blend was hot mixed and pressed under a compression force up to 151 MPa. Green bricks were baked for 2 h at temperatures up to 1000 °C. Voids in the baked bodies were filled with carbon by multiple impregnations using low-softening point coal tar pitch. Each impregnation step (30 min) was followed by calcination at 1000 °C. Brick samples containing 8–12 wt.% coal tar pitch binder and pressed under 108–151 MPa acquired quantify crushing strength. However, multi-impregnating favored the mechanical strength of the baked brick samples and improved their hydration resistance (>45 days). Dolomite brick samples containing 10 wt.% coal tar pitch and pressed at 108 MPa gave high hydration resistance (more than 60 days in normal condition) compared to the hydration resistance of the commercial bricks (30 days). The prepared brick samples have acceptable density, chemical stability, outstanding resistance and good mechanical properties that would meet the requirements of ladle furnace (LF) for steel-making industry.

Sintering behavior and hydration resistance of reactive dolomite was studied by Ghosh and Tripathi [80]. The hydroxide derived from dolomite was developed through precalcination of dolomite followed by its hydration. For hydroxide development, after precalcination, one sample was air-quenched and the other powder was furnace cooled before hydration. The air-quenched samples showed better densification than that of the furnace cooling process at the same temperature. Fe_2O_3 addition enhances sintering by liquid formation at higher temperature. The grain size of doloma with Fe_2O_3 addition is bigger than that without additive. Hydration resistance was related to densification and grain size of sintered dolomite.

The effect of natural dolomite admixtures on calcium zirconate–periclase materials microstructure evolution was studied by Szczerba and Pędzich [71]. In the materials synthesized from natural dolomites and ZrO_2, two main phases were present – calcium zirconate and periclase. During firing of $CaZrO_3$–MgO materials at lower temperatures, the presence of transient phases was detected (mainly ferrites and calcium aluminates, $4CaO–Al_2O_3–Fe_2O_3$ or $2CaO–Fe_2O_3$). These phases disappeared at higher temperatures. This is probably related to the dissolution of impurities in the main phases of $CaZrO_3$–MgO. The material obtained from the mixture of zirconium oxide and natural dolomite with the high impurities content has the highest densification level at 1500 and 1600 °C.

Díaz et al. [48] have studied the evolution of the phases and microstructure as a function of temperature and the processing route of alumina-rich refractory concretes elaborated from spinel, periclase and dolomite. Some authors have studied room temperature mechanical properties of high alumina refractory castables with spinel, periclase and dolomite additions [61]. The mechanical properties of refractory castables at room temperature are critical parameters for selecting suitable operating conditions for the structural design of refractory components. Bending strength studies at room temperature under several thermal treatments and the analysis of the elastic modulus of the refractories and their matrices point to two different mechanical behaviors. From room temperature to 1000 °C, the refractory castables present a pronounced non-linear stress–strain behavior both in the uniaxial tensile and compressive modes, as a result of damage to the microcrack network. Above 1000 °C, the refractory castables begin to sinter owing to a transitory liquid phase, the crystallization of calcium aluminate cement phases and the self-forming spinel phase. At higher firing temperatures, the sintering process leads to a strengthening of the mechanical properties.

Corrosion behavior of $MgO/CaZrO_3$ refractory matrix by clinker was studied by Serena et al. [39]. The attack mechanism to substrates of 80% MgO and 20% $CaZrO_3$ (wt.%) obtained from dolomite and ZrO_2 mixtures and MgO and presintetized $CaZrO_3$ mixtures is established. The studied matrix presented a clinker layer with good adherence that could prevent the corrosion of the refractory brick in work conditions, improving the corrosion resistance. The good corrosion behavior of the studied materials supports their use as a matrix in magnesia chrome-free bricks for the burning zone of rotary cement kilns.

Kalpakli et al. [31] have studied the effect of binder type and other parameters in synthesis of magnesite chromite refractories from process waste. The results of the experiments revealed the optimum type and content of the bond as $MgSO_4{\cdot}7H_2O$ and 8%, and optimum pressing pressure of the materials containing raw magnesite at 250 MPa. It was observed that when the chromite content of the material composition increased from 10% to 28% and 50%, the cold crushing strength (CCS) of the material has decreased, yet its porosity (*P*%) increased. This improves when the sintering temperature increased from 1450 to 1550 °C and 1750 °C. Four spinel-containing matrix compositions in the high-alumina region of the Al_2O_3–MgO–CaO ternary diagram were selected and prepared by using dolomite additions. The creep behavior of these matrices was studied in the temperature interval ranging from 1000 to 1400 °C [58].

6. Conclusion

Basic ceramics are an important class of refractories materials that enable processes to exploit extreme environments. In

recent decades, tremendous efforts have been devoted to innovative processing of basic refractory ceramics and investigation of properties and their application in suitable fields. Because of the large number of papers in this field, this review mainly focuses on the processing and special conditions of the research works. Different processing routes for refractories ceramics have been developed for specific applications to satisfy the associated requirements for porosity, refractoriness, flexural strength and thermal properties. This paper provides a historical perspective on the elaboration of basic refractory from magnesite and dolomite, reviews typical processing routes and summarizes the properties of these materials.

References

[1] C. Sadik, I. El Amrani and A. Albizane, J. Asian Ceram. Soc., 2, 83–96 (2014).
[2] R.A. Landy, in Refractories Handbook, Ed. by C.A. Schacht, (2004) pp. 109–149.
[3] M. Kolli, M. Hamidouche, G. Fantozzi and J. Chevalier, Ceram. Int., 33, 1435–1443 (2007).
[4] C. Sadik, I. El Amrani and A. Albizane, J. Asian Ceram. Soc., 1, 351–355 (2013).
[5] J.D. Smith and W.G. Fahrenholtz, in Refractory Oxides in Ceramic and Glass Materials: Structure, Properties and Processing, Ed. by J.F. Shackelford and R.H. Doremus, (2008) pp. 87–110.
[6] A.P. Reifenstein, H. Kahraman, C.D.A. Coin, N.J. Calos, G. Miller and P. Uwins, Fuel, 78, 1449–1461 (1999).
[7] N. Arvanitidis, J. Geochem. Expl., 62, 217–227 (1998).
[8] D. Sheila, Int. J. Miner. Process., 37, 73–88 (1993).
[9] R.M. Mclntosh, J.H. Sharp and F.W. Xilburn, Thermochim. Acta, 165, 281–296 (1990).
[10] D.M. Ibrahim, A.M. Kabish and N. Ghoniem, Thermochim. Acta, 75, 43–50 (1984).
[11] H. Khalifa and A.I. Atalla, Microchem. J., 20, 299–304 (1975).
[12] E. Barodi, A. Belkasmi, H. El Abdouni and A. El Ouazzani, Les roches et minéraux industriels au Maroc. Chronique de la recherche minière, vols. 531–532 (1998), pp. 139–153.
[13] ASTM C326-03, Standard Test Method for Drying and Firing Shrinkages of Ceramic Whiteware Clays, 15-02, Glass Ceramics (2006).
[14] ASTM C373-88, Standard Test Method for Water Absorption, Bulk Density, Apparent Porosity, and Apparent Specific Gravity of Fired Whiteware Products, 15-02, Glass Ceramics (2006).
[15] ASTM C674-88, Standard Test Methods for Flexural Properties of Ceramic White-Ware Materials, 15-02, Glass Ceramics (2006).
[16] A.V. Gal'yanov, Yu.V. Laptev, M.N. Kovalev and A.I. Vladimirov, Refract. Ind. Ceram., 41, 245–248 (2000).
[17] E. Alvarado, L.M. Torres-Martinez, A.F. Fuentes and P. Quintana, Polyhedron, 19, 2345–2351 (2000).
[18] J. Warren, Earth-Sci. Rev., 52, 1–81 (2000).
[19] A. Tsirambides, Mater. Struct., 34, 110–113 (2001).
[20] O.F. Shatilov, V.G. Karelin, Yu.F. Gogolev, V.N. Koptelov and A.P. Baranov, Refract. Ind. Ceram., 42, 41–44 (2001).
[21] A.V. Gropyanov and V.M. Gropyanov, Refract. Ind. Ceram., 42, 162–165 (2001).
[22] I.D. Kashcheev, Refract. Ind. Ceram., 42, 288–293 (2001).
[23] M. Samtani, E. Skrzypczak-Janktun, D. Dollimore and K. Alexander, Thermochim. Acta, 367–368, 297–309 (2001).
[24] M.F.M. Zawrah, Ceram. Int., 27, 523–529 (2001).
[25] N.M.A. Khalil, S.A.S. El-Hemaly and L.G. Girgis, Ceram. Int., 27, 865–873 (2001).
[26] H.H.M. Darweesh, Ceram. Int., 27, 45–50 (2001).
[27] K. Sato and T. Katsura, Earth Planet. Sci. Lett., 184, 529–553 (2001).
[28] M. Samtani, D. Dollimore, F.W. Wilburn and K. Alexander, Thermochim. Acta, 367–368, 285–295 (2001).
[29] F.N. Cunha-Duncan and R.C. Bradt, J. Am. Ceram. Soc., 85, 2995–3003 (2002).
[30] D.U. Tulyaganov, M.E. Tukhtaev, J.I. Escalante, M.J. Ribeiro and J.A. Labrincha, J. Eur. Ceram. Soc., 22, 1775–1782 (2002).
[31] Y.K. Kalpakli, S. Gökmen and S. Özgen, J. Eur. Ceram. Soc., 22, 755–759 (2002).
[32] M.A. Serry, M.B. El-Kholi, M.S. Elmaghraby and R. Telle, Ceram. Int., 28, 575–583 (2002).
[33] E. Mustafa, N. Khalil and A. Gamal, Ceram. Int., 28, 663–667 (2002).
[34] M. Samtani, D. Dollimore and K.S. Alexander, Thermochim. Acta, 392–393, 135–145 (2002).
[35] I.D. Kashcheev, V.A. Kamenskikh, K.G. Zemlyanoi, O.F. Shatilov, V.N. Koptelov and D.V. Ponomarev, Refract. Ind. Ceram., 44, 301–305 (2003).
[36] F. Demir, B. Donmez, H. Okur and F. Sevim, Chem. Eng. Res. Des., 81, 618–622 (2003).
[37] D.T. Beruto, R. Vecchiattini and M. Giordani, Thermochim. Acta, 405, 183–194 (2003).
[38] G.I. Antonov, V.P. Nedosvitii, A.S. Kulik and O.M. Semenenko, Refract. Ind. Ceram., 45, 160–164 (2004).
[39] S. Serena, M.A. Sainz and A. Caballero, J. Eur. Ceram. Soc., 24, 2399–2406 (2004).
[40] H.A. Yeprem, E. Türedi and S. Karagöz, Mater. Charact., 52, 331–340 (2004).
[41] M.K. Haldar, H.S. Tripathi, S.K. Das and A. Ghosh, Ceram. Int., 30, 911–915 (2004).
[42] G. Chen and D. Tao, Int. J. Miner. Process., 74, 343–357 (2004).
[43] S.A. Suvorov, M.I. Nazmiev, A.P. Baranov and A.A. Dmitrienko, Refract. Ind. Ceram., 46, 217–219 (2005).
[44] C. Aksel, F. Kasap and A. Sesver, Ceram. Int., 31, 121–127 (2005).
[45] P. Maravelaki-Kalaitzaki, A. Bakolas, I. Karatasios and V. Kilikoglou, Cement Concr. Res., 35, 1577–1586 (2005).
[46] A.G.M. Othman and W.M.N. Nour, Ceram. Int., 31, 1053–1059 (2005).
[47] O.S. Pokrovsky, S.V. Golubev and J. Schott, Chem. Geol., 217, 239–255 (2005).
[48] L.A. Díaz, R. Torrecillas, A.H. De Aza, P. Pena and S. De Aza, J. Eur. Ceram. Soc., 25, 1499–1506 (2005).
[49] X. Lingling and D. Min, Cement Concr. Res., 35, 1480–1485 (2005).
[50] T.I. Shchekina, E.N. Gramenitskii, A.M. Batanova, T.A. Kurbyko, A.V. Likhodievskii, B.N. Grigor'ev, A.N. Pyrikov, O. Sheshevichka and R. Gazhur, Refract. Ind. Ceram., 47, 363–372 (2006).
[51] N.F. Solodkii and A.S. Shamrikov, Glass Ceram., 63, 298–304 (2006).
[52] G. Ye and T. Troczynski, Ceram. Int., 32, 257–262 (2006).
[53] O. Kanga and A. Guney, Miner. Eng., 19, 376–378 (2006).
[54] C.A.R. González, W.F. Caley and R.A.L. Drew, Metall. Mater. Trans. B, 38, 167–174 (2007).
[55] A. Ghosh, M.K. Haldar and S.K. Das, Ceram. Int., 33, 821–825 (2007).
[56] H.A. Yeprem, J. Eur. Ceram. Soc., 27, 1651–1655 (2007).
[57] E. Mako, J. Eur. Ceram. Soc., 27, 535–540 (2007).
[58] L.A. Díaz and R. Torrecillas, J. Eur. Ceram. Soc., 27, 67–72 (2007).
[59] S. Kurama, A. Kara and H. Kurama, J. Eur. Ceram. Soc., 27, 1715–1720 (2007).
[60] Y.K. Kalpakli, Refract. Ind. Ceram., 49, 314–319 (2008).
[61] L.A. Díaz, R. Torrecillas, F. Simonin and G. Fantozzi, J. Eur. Ceram. Soc., 28, 2853–2858 (2008).
[62] G. Peiwei, L. Xiaolin, J. Shaochun, Z. Hui and G. Chunxing, Mater. Lett., 62, 106–108 (2008).
[63] L.M. Aksel'rod, A.P. Laptev and A.A. Shlyapin, Refract. Ind. Ceram., 49, 1–4 (2008).
[64] Yu.V. Prokof'ev, O.N. Zakharov and P.B. Razgovorov, Glass Ceram., 66, 147–150 (2009).
[65] M. Rabah and E.M.M. Ewais, Ceram. Int., 35, 813–819 (2009).
[66] S.M. Siadati and A. Monshi, Ceram. Int., 35, 2845–2852 (2009).
[67] A.G. Tomba Martinez, M.A. Camerucci, A.L. Cavalieri, L. Martorello and P.G. Galliano, J. Eur. Ceram. Soc., 29, 581–586 (2009).
[68] P. Adriano, A. Santos Silva, R. Veiga, J. Mirão and A.E. Candeias, Mater. Charact., 60, 610–620 (2009).
[69] K. Das, S. Mukherjee, P.K. Maiti and P.G. Pal, Bull. Mater. Sci., 33, 439–444 (2010).
[70] O. Yamamoto, T. Ohira, K. Alvarez and M. Fukuda, Mater. Sci. Eng. B, 173, 208–212 (2010).
[71] J. Szczerba and Z. Pędzich, Ceram. Int., 36, 535–547 (2010).
[72] M.I. Mahadi and S. Palaniandy, Int. J. Miner. Process., 94, 172–179 (2010).
[73] M. Hojamberdiev, P. Arifov, K. Tadjiev and Y. Xu, Miner. Sci. Technol., 20, 415–420 (2010).
[74] M. Hojamberdiev, P. Arifov, K. Tadjiev and Y. Xu, Int. J. Miner. Metall. Mater., 18, 105–114 (2011).
[75] G.A. Khater, Ceram. Int., 37, 2193–2199 (2011).
[76] Á. Obregón, J.L.R. Galicia, J.L. Cuevas, P. Pena and C. Baudín, J. Eur. Ceram. Soc., 31, 61–74 (2011).
[77] G.A. Khater and M.M. Morsi, Thermochim. Acta, 519, 6–11 (2011).
[78] A.M. Urvantsev and I.D. Kashcheev, Refract. Ind. Ceram., 53, 78–81 (2012).
[79] X.W. Liu, Y.L. Feng, H.R. Li, P. Zhang and P. Wang, J. Therm. Anal. Calorim., 107, 407–412 (2012).
[80] A. Ghosh and H.S. Tripathi, Ceram. Int., 38, 1315–1318 (2012).
[81] S. Dwarapudi, T.K. Ghosh, V. Tathavadkar, M.B. Denys, D. Bhattacharjee and R. Venugopal, Int. J. Miner. Process., 112–113, 55–62 (2012).
[82] P.G. Lampropoulou, C.G. Katagas, I. Iliopoulos and D. Papoulis, Refract. Ind. Ceram., 53, 310–316 (2013).
[83] M.H. Cho, T.Y. Mun and J.S. Kim, Energy, 53, 299–305 (2013).
[84] C.A. Macris, E.D. Young and C.E. Manning, Geochim. Cosmochim. Acta, 118, 18–32 (2013).
[85] A.G.M. Othman, Br. Ceram. Trans., 102, 265–271 (2013).
[86] K. Sasaki, X. Qiu, Y. Hosomomi, S. Moriyama and T. Hirajima, Microporous Mesoporous Mater., 171, 1–8 (2013).
[87] X. Wang, Z. Bai, D. Zhao, Y. Chai, M. Guo and J. Zhang, Mater. Res. Bull., 48, 1228–1232 (2013).
[88] L. Tian, A. Tahmasebi and J. Yu, J. Therm. Anal. Calorim., 118, 1577–1584 (2014).
[89] A.M. Soltan, M. Wendschuh, H. Willims and M. Serry, J. Eur. Ceram. Soc., 34, 2023–2203 (2014).
[90] G. Charalampides, K.I. Vatalis, S. Platias and V. Karayannis, Proc. Econ. Finance, 14, 128–136 (2014).
[91] D. Fu, N. Feng, Y. Wang, J. Peng and Y. Di, Trans. Nonferrous Metals Soc. China, 24, 839–847 (2014).
[92] Q. Gao, G. Wei, X. Jiang, H. Zheng and F. Shen, J. Iron Steel Res. Int., 21, 408–412 (2014).
[93] R.D.V. Zermeño, J. Formosa, J.A. Aparicio and J.M. Chimenos, Chem. Eng. J., 254, 63–72 (2014).
[94] Y. Huang, R. Kang, X. Ma, Y. Qi, J. Mulder and L. Duan, Sci. Total Environ., 481, 469–478 (2014).
[95] D. Fu, Y. Wang, J. Peng, Y. Di, S. Tao and N. Feng, Trans. Nonferrous Metals Soc. China, 24, 2677–2686 (2014).

[96] C. Ghosh, A. Ghosh, H.S. Tripathi, J. Ghosh and M.K. Haldar, Ceram. Int., 40, 16791–16798 (2014).
[97] G. Gadikota, C. Natali, C. Boschi and A.A. Park, J. Hazard. Mater., 264, 42–52 (2014).
[98] X. Zhang, F.P. Glasser and K.L. Scrivener, Cement Concr. Res., 66, 11–18 (2014).
[99] Z. Liu, S. Wang, J. Huang, Z. Wei, B. Guan and J. Fang, Constr. Build. Mater., 85, 247–255 (2015).
[100] P. Kumar, Burhanuddin, A. Kumar, A. Ghosh, S. Sinhamahapatra and H.S. Tripathi, Ceram. Int., 41, 9003–9008 (2015).
[101] A.E. Lavat, M.C. Grasselli and E.G. Lovecchio, Ceram. Int., 41, 2107–2115 (2015).
[102] İ. Kıpçak and T.G. Isıyel, Korean J. Chem. Eng., 32, 1634–1641 (2015).
[103] L. Chen, G. Ye, Q. Wang, B. Blanpain, A. Malfliet and M. Guo, Ceram. Int., 41, 2234–2239 (2015).
[104] K. Wang, D. Han, P. Zhao, X. Hu, Z. Yin and D. Wu, Thermochim. Acta, 614, 199–206 (2015).
[105] L. Chen, G. Ye, W. Zhou, J. Dijkmans, B. Sels, A. Malfliet and M. Guo, Ceram. Int., 41, 12651–12657 (2015).
[106] W. Yan, J. Chen, N. Li, W. Qiu, Y. Wei and B. Han, Ceram. Int., 41, 515–520 (2015).
[107] F. Wang, J. Ye, G. He, G. Liu, Z. Xie and J. Li, Ceram. Int., 41, 7374–7380 (2015).
[108] E. Thomaidis and G. Kostakis, Ceram. Int., 41, 9701–9707 (2015).
[109] A.A. Albhilil, M. Palou, J. Kozánková and M. Boháč, Arab. J. Sci. Eng., 40, 151–161 (2015).
[110] R.T. da Cruz and S.R. Bragança, Ceram. Int., 41, 4775–4781 (2015).
[111] H. Temiz, F. Kantarcı and M.E. İnceer, Constr. Build. Mater., 94, 528–535 (2015).
[112] Burhanuddin, A. Kumar, P. Kumar, A. Ghosh, S. Sinhamahapatra and H.S. Tripathi, Int. J. Miner. Process., 144, 40–45 (2015).
[113] F.N. Booth, L.B. Garrido and E.F. Aglietti, Proc. Mater. Sci., 8, 172–179 (2015).
[114] N. Raza, Z.I. Zafar, N.U. Haq and R.V. Kumar, Int. J. Miner. Process., 139, 25–30 (2015).
[115] D. Dębska, Proc. Eng., 108, 673–680 (2015).
[116] L.P. Li, Y. Yan, X.Z. Fan, Z.H. Hu and C.Y. Zhao, J. Eur. Ceram. Soc., 35, 2923–2931 (2015).
[117] J. Formosa, A.M. Lacasta, A. Navarro, R.V. Zermeño, M. Niubó, J.R. Rosell and J.M. Chimenos, Constr. Build. Mater., 91, 150–157 (2015).
[118] D. Sifré, L. Hashim and F. Gaillard, Chem. Geol., 418, 189–197 (2015).
[119] J.J. Xie, T. Chen, B. Xing, H. Liu, Q. Xie, H. Li and Y. Wu, Appl. Clay Sci., 119, 42–48 (2016).
[120] L. Chen, A. Malfliet, P.T. Jones, B. Blanpain and M. Guo, Ceram. Int., 42, 743–751 (2016).
[121] Q. Gautier, P. Bénézeth and J. Schott, Geochim. Cosmochim. Acta, 181, 101–125 (2016).
[122] V. Masindi and W.M. Gitari, J. Clean. Prod., 112, 1077–1085 (2016).
[123] V. Masindi, M.W. Gitari, H. Tutu and M. DeBeer, J. Water Process. Eng., (2016) (in press).
[124] C. Richmond, in Refractories Handbook, Ed. by C.A. Schacht, (2004) pp. 183–200.